

# Microstructures Comparison of Stellite 6 Alloy by Self-Propagating High-Temperature Synthesis and Cast HS111 Alloy

Xu Yangtao, Xia Tiandong, Huang Yanling

State Key Laboratory of Gansu Advanced Non-ferrous Metal Materials, Lanzhou University of Technology, Lanzhou 730050, China

**Abstract:** The microstructures of as-SHSed Stellite 6 and as-cast HS111 were investigated by SEM, XRD and EPMA. It was shown that there is significant similarity in the microstructures of as-SHSed Stellite 6 and as-cast HS111. But carbides of continuous cast HS111 alloy can form single and uniform carbides phase.

**Key words:** SHS; cobalt-base alloy Stellite 6; microstructure

Cobalt-base super-alloys were found in the early 1900s. After that, the Stellite alloys have effected important industrial materials for example cutlery, machine tools and wear-resistant hard facing applications<sup>[1]</sup>. The recent discovery of the stable ternary  $\text{Co}_3(\text{Al,W})$  intermetallic compound with a close-packed  $\text{L}_{12}$  structure<sup>[2]</sup> provides a pathway for development of a new class of load-bearing, cobalt-base high-temperature alloys. This novel Co-Al-W based alloy system reinforced with high volume fractions of the  $\text{L}_{12}$  compound offers new possibilities for application in severe environments (above 1173 K), such as in industrial combined cycle power-generation systems, and has a great promise as candidates for next-generation high-temperature materials<sup>[3]</sup>.

Stellite 6 with nominal composition Co-28Cr-4.5W-1.2C was the first Stellite alloy developed in the early 1900s by Elwood Haynes. In recent years there have been investigations on the effect of additions of alloying elements<sup>[4-6]</sup> on the microstructure and mechanical properties of Stellite 6. It has been shown that addition of W and Mo will influence the corrosion behavior by stabilizing the face centered cubic (fcc) phase<sup>[7]</sup>. Solid solution strengthening of Co-base alloy is normally provided by adding of tantalum, tungsten, molybdenum, chromium and columbium<sup>[1]</sup>. Currently, the use of Stellite alloys has extended into various industrial sectors such as pulp and

paper processing, oil and gas processing, pharmaceuticals, chemical processing, and the need for improving of Stellite alloys has increased. It has been recognized that processing will affect the microstructure of Stellite alloy<sup>[8]</sup>.

Combustion synthesis, or self-propagating high temperature synthesis (SHS), relies on the ability of highly synthesis reaction, the exothermic reactions to be self-sustaining. Compared with conventional processing methods, combustion synthesis has the following advantages: the simple exothermic nature of the process avoids the need for expensive processing facilities and equipment; the short processing time results in low operating and processing costs, and so on. Because of these advantages of the process, it is possible to produce novel materials with improved mechanical, electrical, optical, and chemical properties, such as high-temperature intermetallics and composite materials.

It is well known that the nominal chemical composition of cobalt-base alloy Stellite 6 and HS111 alloy have similar content of all kinds of primary elements such as cobalt, chromium and tungsten; moreover, both them are used as important industrial materials. The focus of this work is to compare the microstructures of a cobalt-base alloy Stellite 6 manufactured by SHS with HS111 alloy by continuous casting process.

Received date: July 27, 2008; Revised manuscript received date: July 1, 2009

Foundation item: Supported by West Light Foundation of the Chinese Academy of Sciences

Biography: Xu Yangtao, Candidate for Ph. D., Lecturer, School of Materials Science and Engineering, Lanzhou University of Technology, Lanzhou 730050, P. R. China, Tel: 0086-931-2973563, E-mail: [xuyt@lut.cn](mailto:xuyt@lut.cn)

Copyright © 2009, Northwest Institute for Nonferrous Metal Research. Published by Elsevier BV. All rights reserved.

## 1 Experimental

Elemental powders of tungsten (0.98 μm, 99.8% purity), aluminum (3.59 μm, 99.5% purity), cobalt oxide (Co<sub>3</sub>O<sub>4</sub>) (4.5 μm, 99.0% purity) and carbon (<30 μm, 99% purity) were used as starting materials. The powders were mixed by ball mill (ratio of the ball to starting powders was 1.3:1, time 90 min and rotation speed 800 r/min). 30 grams of mixed reactant powders were pressed into a pellet, and subsequently ignited by tungsten inert gas (TIG) arc welding in the graphite crucible. Commercial HS111 by continuous casting process was used as comparison sample. These alloys are hereafter referred to as SHSed Stellite 6 and HS111 alloy, respectively.

The chemical composition of both samples measured by EDXRF analysis is given in Table 1. The phases were examined and analyzed using the electron probe microscopy analysis (EPMA). XRD analyses were performed on the Rigaku D/max-IIIB X-ray diffractometer with a Cu Kα radiation (λ=0.15406 nm), operating at 40 kV and 20 mA. The scanning speed was 4°min<sup>-1</sup>.

Optical microscopy and scanning electron microscopy (SEM) were used in the initial stages of the program for characterization of the materials in the as-received conditions. The microstructure and the size and distribution of the carbides were assessed for both alloys. The samples for SEM observation were etched electrolytically in a solution consisting of 5% perchloric acid in methanol at about 20 °C. The SEM used in this study is equipped with a LaB6 gun, and is capable of operating as a conventional high-vacuum SEM. It is fully equipped with a range of secondary electron (SE) and back-scattered electron (BSE) detectors.

## 2 Results

Fig.1 shows the shape of the sample ignited by tungsten inert gas (TIG) arc welding. The density of SHSed Stellite 6 alloy is about 8.5 g/cm<sup>3</sup> and the residual Al<sub>2</sub>O<sub>3</sub> about 2.8 g/cm<sup>3</sup>; obviously, the residual has been separated from SHSed Stellite 6 alloy and floated on the surface of the sample.

**Table 1** Chemical compositions of SHSed Stellite 6 and HS111 alloy

Manufacturing technique	Mass fraction/%									
	Co	Cr	W	Fe	Mn	Mo	Ni	Al	C	Si
SHSed Stellite 6	55.85	28.52	3.93	3.70	0.47	0.92	2.78	1.48	1.26	1.09
HS111 alloy	55.39	28.50	4.52	4.43	1.94	—	2.60	—	0.84	1.78
Original Stellite 6	55.47	28.70	3.90	4.20	0.30	3.26	1.60	—	1.57	1.00

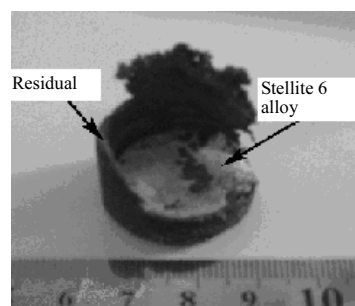


Fig.1 Shape of the sample by combustion synthesis

Fig.2 shows the optical micrographs of the HS111 alloy (a) and (b), SHSed Stellite 6 alloy (c) and (d). Cobalt-base superalloys consist of a continuous fcc matrix and a variety of carbides, mainly coarse primary  $M_{23}C_6$ ,  $M_7C_3$  and  $MC$ . A “light” phase has fcc structure and etched difficulty, as a nobler phase. On the contrary, a “dark” phase is etched more easily, as a less noble phase that has hcp-structure<sup>[9]</sup>. The first phase to form during cooling from the liquid state of the Stellite 6 alloy produced by SHS processing is the primary Co-rich dendrite and the remaining liquid eventually solidifies into an interdendritic, intimate lamellar mixture of Co-rich phase and Cr-rich carbides<sup>[10]</sup> by a eutectic reaction.

The carbides contribute significantly to strengthening the rich  $\gamma$ -Co matrix. The carbides form upon alloys cooling down in shell mold. They precipitate at grain boundaries and in interdendritic regions. During service at high temperature, secondary carbides usually are  $M_{23}C_6$ , precipitates. The fine secondary carbide pins up dislocations that hardens the matrix. Obviously, the morphology, distribution and size of the secondary carbides will affect precipitation hardening effect<sup>[11]</sup>.

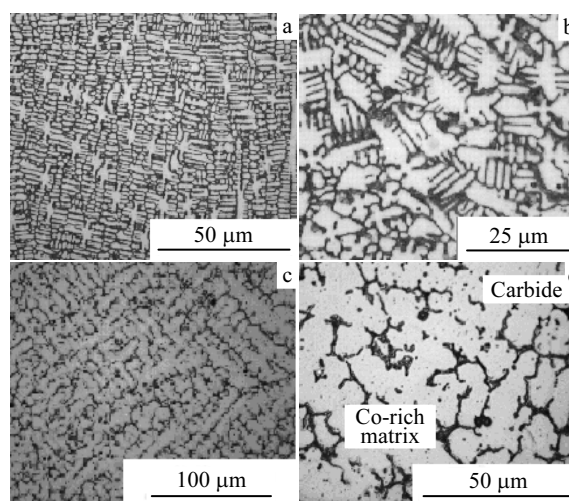


Fig.2 Micrographs of HS111 alloy (a) and (b), SHSed Stellite 6 alloy (c) and (d), the carbides (dark gray) and Co-rich matrix (light gray)

Fig.3 shows the morphologies and distribution of the carbide phases of HS111 alloy (a) and SHSed Stellite 6 alloy (b). In this backscattered electron image, the chromium-rich  $Cr_7C_3$  carbide displays dark color and the CrC carbide rather light. It is observed that  $Cr_7C_3$  carbide is in the form of rods or irregular aggregates, while CrC is present as a discrete, blocky dispersion with well-distributed Chinese script morphology. Such a morphology of CrC is also observed in the as-cast DZ40M alloy<sup>[11]</sup>. Evidently, the formation of CrC is attributed to the addition of reactive elements Ta, Ti and Zr. Both the  $Cr_7C_3$  and CrC carbides are located at grain boundaries or in interdendritic regions, forming a continuous network around the columnar grained matrix.

In the continuous casting process of HS111 alloy, the microstructure consists of  $\gamma$ -Co solid solution (light region) and an interdendritic eutectic comprising  $\gamma$ -Co solid solution with  $M_7C_3$  carbides. In contrast, the SHSed Stellite 6 comprises spheroidal carbides with average dimension 5  $\mu$ m, which are uniformly distributed in the  $\gamma$ -Co matrix.

Fig.4 and Fig.5 show the semi-quantitative analysis of SHSed Stellite 6 and HS111 alloy for localized regions, respectively. Measured chemical composition of the SHSed Stellite 6 and the HS111 alloy localized regions by EPMA are presented in Table 2 and 3. From the specific carbide (Fig.4 point 2 and Fig.5 point 1) and matrix (Fig.4 point 1 and Fig.5 point 2), it is noted that primary elements of the points have the approximately same content, respectively, such as cobalt, chromium and tungsten. That is to say, the carbides types and form are analogical. In agreement with other papers<sup>[12]</sup>, the matrix was found to be Co-rich and the carbides Cr-rich, although there is evidence to suggest there are other elements in the carbide phase.

From Fig.4 and Table 2, it is also concluded that the primary phase of point 1 is  $\gamma$ -Co matrix, in respect that cobalt content is distinctly much higher than the others. The carbon content of point 2 and the oxygen content of point 6 exceed the other points, respectively. Consequently, we identified that the white point was aluminum oxidation ( $Al_2O_3$ ), because the liquid alloy has not kept enough time

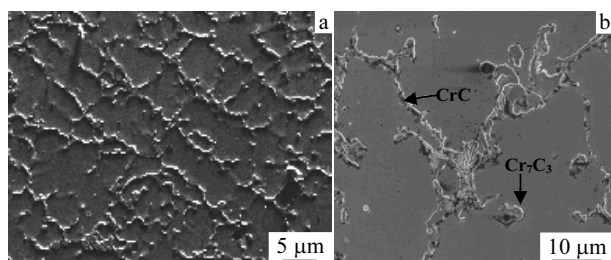


Fig.3 Micrographs of the carbides of HS111 alloy (a) and SHSed Stellite 6 alloys (b) (light gray is the carbides, and dark gray is the Co-rich matrix)

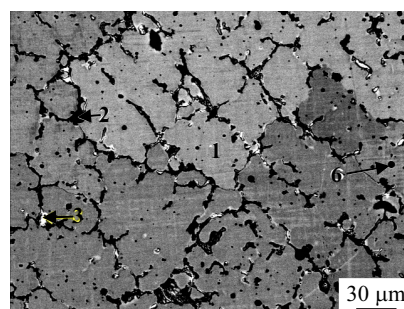


Fig.4 The semi-quantitative analysis of SHSed Stellite 6 alloy for localized regions (point)

Table 2 Measured chemical composition of SHSed Stellite 6 localized regions by EPMA

Point	Mass fraction/%									
	Co	Cr	W	Fe	Ni	Mo	Al	C	Si	O
1	62.387	24.01	—	4.019	3.663	—	1.531	4.390	—	—
2	35.091	33.537	5.746	2.695	—	2.094	0.774	19.054	1.009	—
3	42.542	27.031	12.213	2.788	—	4.237	0.965	7.975	2.249	—
6	5.340	4.327	—	—	—	—	—	—	—	57.072

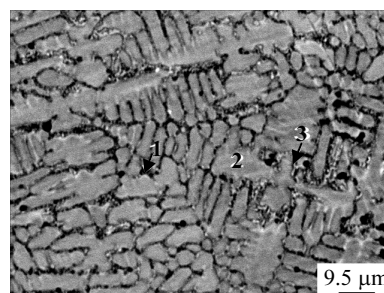


Fig.5 The semi-quantitative analysis of HS111 alloy for localized regions (point)

Table 3 Measured chemical composition of HS111 localized regions by EPMA

Point	Mass fraction/%								
	Co	Cr	W	Fe	Mo	Ni	C	Si	O
1	28.105	32.584	8.188	2.903	1.041	2.173	9.723	0.996	—
2	42.779	19.527	—	4.250	—	3.112	5.522	1.208	—
3	50.730	32.513	6.464	4.703	1.639	3.979	—	1.611	—

on SHS processing. So, the residual is mainly aluminum oxidation ( $Al_2O_3$ ) and locates on the interface. In the same way, from Fig.5 and Table 3, we can draw that point 2 is  $\gamma$ -Co matrix, point 1 is carbides and point 3 is intermetallics.

Fig.6 shows XRD patterns of HS111 alloy (a), SHSed Stellite 6 alloy (b) and the residual (c). XRD analysis shows a substantial contrast in the relative intensities of the  $2\theta$  peaks for the HS111 alloy (Fig. 6a) and SHSed Stellite 6 alloy (Fig. 6b). As far as possible, the different phases have been identified using the indexing facility on the MDI

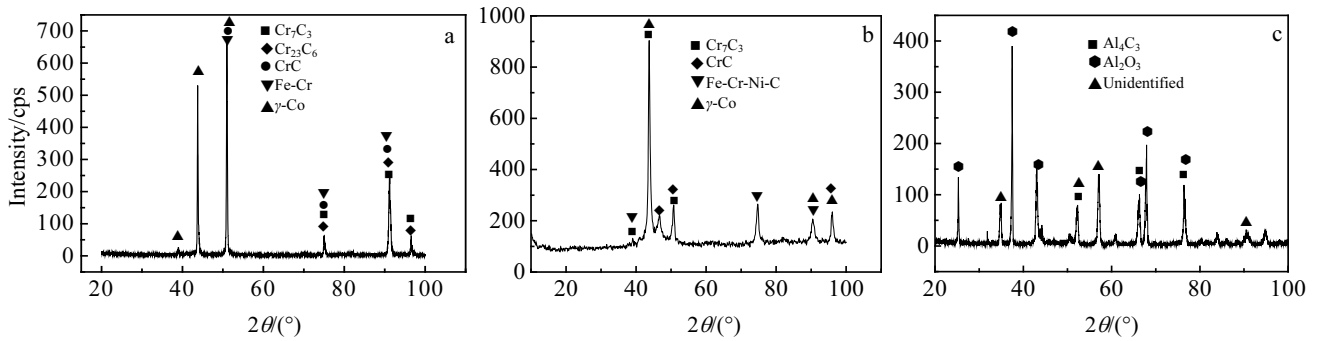


Fig.6 XRD patterns of (a) cast HS111 alloy, (b) SHSed Stellite 6 alloy, and (c) the residual

Jade software. The samples include a large number of carbides such as  $Cr_7C_3$  and  $Cr_{23}C_6$ , which are basically chromium carbides containing cobalt in substitution from chromium and  $MC$  carbides. From Fig.6c, we can conclude that the residual consisted of aluminum oxidation ( $Al_2O_3$ ) and other complicated compounds, which are resulted from the exothermic reaction.

Upon comparing Fig.6a with 6b, it can be seen that the sample of SHSed Stellite 6 has never undergone heat-treatment and as a result the phase composition is relatively complicated and carbides ( $MC$ ) phase transformation have not changed. Because solidification rate  $R$  of the SHS processing Stellite 6 is much higher than that of the continuous casting process (HS111), some non-equilibrium phase can exist in SHS at high temperature. Nevertheless, the continuous casting process (HS111) can sustain lower solidification speed. Accordingly, under this condition, metastable phase could not exist long, and the carbides of continuous casting HS111 alloy will change into pure and uniform carbides phases.

### 3 Discussions

The chemical compositions of SHSed Stellite 6 and the HS111 alloy are very similar, so it is necessary to observe and analyze the type, size, shape and amount of carbides formed after these processing methods. In literatures, two main types of carbides have been reported for cobalt-based alloys. They are chromium-rich carbides ( $Cr_3C_2$ ,  $Cr_7C_3$  and  $Cr_{23}C_6$ ) and refractory-element-rich carbides ( $M_6C$  and  $MC$ ). In this paper, a small quantity of carbides and intermetallics show atomic formula of Fe-Cr-Ni-C of the SHS process (Stellite 6) because of the specimen's un-heat-treatment. Domalavage<sup>[13]</sup> suggested a transformation of  $M_7C_3$  and  $M_{23}C_6$  during ageing in Stellite X40 casting as follows:



This demonstrates that a non-equilibrium structure can exist in Co castings at high temperatures. Zhuang and Langer<sup>[14]</sup> reported that in cast Co-Cr-Mo alloys, the com-

position of the carbides depends on the process conditions. By changing the cooling rate, they found that the chemical composition of carbide particles and the crystal structure will change to a certain extent.

Considering the work reported in the literature, it would be found that the carbides formed during SHS processing and continuous casting process would differ in the chemical composition, crystal structure and the physical morphology indeed. This is confirmed by microscopy and XRD. The chromium-rich carbides  $Cr_{23}C_6$ ,  $Cr_7C_3$  formed during SHS processing probably have more Cr and the crystal structure is much more stable after heat treatment for SHSed Stellite 6.

### 4 Conclusions

1) The cobalt-rich main matrixes in the HS111 alloy and SHSed Stellite 6 have an unstable fcc structure at room temperature. In SHSed Stellite 6, different kinds of carbides are distributed over the interdendritic regions as granular shapes, not as lamellar eutectic as seen in the original Stellite 6 alloy.

2) Upon comparing the continuous casting process HS111 alloy with SHSed Stellite 6, two specimens have similar microstructure and metastable phase carbides.

### References

- 1 Malayoglu U, Neville A, Beamson G. *Materials Science and Engineering A*[J], 2005, 393: 91
- 2 Sato J, Omori T, Oikawa K et al. *Science*[J], 2006, 312: 90
- 3 Akane Suzuki, Garret C DeNolf et al. *Scripta Materialia*[J], 2007, 56: 385
- 4 Wang Linchun, Li D Y. *Wear*[J], 2003, 255: 535
- 5 Kuzucu V, Ceylan M, Celik H et al. *Journal of Materials Processing Technology*[J], 1997, 69: 257
- 6 Halis Çelik, Mehmet Kaplan. *Wear*[J], 2004, 257: 606
- 7 Hocking W H, Stanchell F W, McAlpine E et al. *Corros Sci*[J], 1985, 25(7): 531
- 8 Malayoglu U, Neville A, Lovelock H. *Corrosion Science*[J], 2005, 47: 1911

- 9 Tanja Matkovic, Prosper Matkovic, Jadranka Malina. *Journal of Alloys and Compounds*[J], 2004, 366: 293
- 10 Jong-Choul Shin, Jung-Man Doh, Jin-Kook Yoon et al. *Surface and Coatings Technology*[J], 2003, 166: 117
- 11 Jiang W H, Guan H R, Hu Z Q. *Materials Science and Engineering A*[J], 1999, 271: 101
- 12 Atamert S. *Comparison of the Microstructure and Abrasive Wear Properties of Stellite Hardfacing Alloys Deposited by Arc Welding and Laser Cladding*[D]. Cambridge: University of Cambridge, 1989
- 13 Domalavage P K. *Assessing the Kinetics and Mechanisms of Corrosion of Cast and HIPed Stellite 6 in Aqueous Saline Environments*[D]. Boston: MIT, 1980
- 14 Zhuang L, Langer E W. *Z Metall*[J], 1989, 80: 251

## 自蔓延高温合成钴基 Stellite 6 合金和铸造 HS111 合金微观组织

徐仰涛, 夏天东, 黄艳灵

(兰州理工大学 甘肃省有色金属新材料省部共建国家重点实验室, 甘肃 兰州 730050)

**摘要:** 运用 SEM、XRD 和 EPMA 等分析方法对自蔓延高温合成钴基 Stellite 6 合金与连续铸造态钴基合金 HS111 的微观组织进行比较研究。结果表明, 运用自蔓延高温合成方法制备的钴基 Stellite 6 合金与连续铸造态的钴基合金 HS111 的微观组织结构相似, 但连铸 HS111 中的碳化物种类比较单一且均匀。

**关键词:** 自蔓延高温合成; 钴基 Stellite 6 合金; 微观组织

---

作者简介: 徐仰涛, 男, 1978 年生, 博士生, 讲师, 兰州理工大学材料科学与工程学院, 甘肃 兰州 730050, 电话: 0931-2973563, E-mail: xuyt@lut.cn